Remote Sensing Applications: Society and Environment 43 (2026) 102200

Contents lists available at ScienceDirect

Remote Sensing Applications: Society and Environment

journal homepage: www.elsevier.com/locate/rsase

Mapping of coffee cultivation based on land use/land cover in the tropics of Cajamarca (Peru): An integration of Sentinel data, machine learning, and Google Earth Engine

Elgar Barboza[a,b,*], Amanda Aragon[c], Samuel Pizarro[b], Alcides Roman[d], Brandon Adams[c], Ellen Delgado[c], Alexander Cotrina-Sanchez[b], Aqil Tariq[e], Angel J. Medina-Medina[b], Katerin M. Tuesta-Trauco[b], Abner S. Rivera-Fernandez[b], Jhon A. Zabaleta-Santisteban[b], Candy Ocaña[f], Marguerite Madden[b,**]

[a] *Facultad de Ingeniería Ambiental, Biosistemas y de la Energía (FIABE), Universidad Nacional Toribio Rodríguez de Mendoza de Amazonas, Chachapoyas, 01001, Peru*

[b] *Instituto de Investigación para el Desarrollo Sustentable de Ceja de Selva (INDES-CES), Universidad Nacional Toribio Rodríguez de Mendoza de Amazonas, Chachapoyas, 01001, Peru*

[c] *Center for Geospatial Research, Department of Geography, University of Georgia, Athens, GA, 30602, USA*

[d] *Estación Experimental Agraria Amazonas, Dirección de Investigación y Desarrollo Tecnológico, Instituto Nacional de Innovación Agraria (INIA), Chachapoyas, 01001, Peru*

[e] *Department of Wildlife, Fisheries and Aquaculture, College of the Forest Resources, Mississippi State University, Starkville, MS, 39762-9690, USA*

[f] *Grupo de Investigación de Sistemas Remotos y Análisis de Datos (SIRANDA), Instituto de Investigación de Ciencia de Datos, Universidad Nacional de Jaén (UNJ), Carretera Jaén San Ignacio KM 21, Jaén, 06801, Peru*

ARTICLE INFO

Keywords:
Sustainable agriculture
Agroforestry systems
Random forest
Tasseled cap transformation
Variance inflation factor

ABSTRACT

Coffee cultivation is a strategic economic activity in the Andean-Amazonian region of Peru, characterized by its diversity of production systems and complex landscape. In this study, a methodological approach based on multitemporal mapping of land cover and land use (LULC) was developed to identify coffee crops by integrating optical satellite imagery (Sentinel-2) and radar data (Sentinel-1), as well as topographic variables, processed on the Google Earth Engine (GEE) platform, with supervised classification based on the Random Forest (RF) algorithm. The study area covered the provinces of Jaen and San Ignacio (Cajamarca), the main coffee-growing areas in the country's north. A time series of satellite data from 2019 to 2024 was used, considering two climatic seasons (dry and wet). The 69 spectral, textural, and topographic variables were evaluated but subsequently reduced to 22 using the Variance Inflation Factor (VIF). The classification distinguished 11 LULC classes, including shade-grown and non-shade-grown coffee, achieving an overall accuracy of over 84% and a Kappa index of 0.90. The binary coffee maps made it possible to quantify and analyze the spatial dynamics of the crop in both provinces, showing a growing trend toward shade-grown coffee, especially in San Ignacio. The proposed approach proved to be operational for mountainous tropical areas with high cloud cover

* Corresponding author. Facultad de Ingeniería Ambiental, Biosistemas y de la Energía (FIABE), Universidad Nacional Toribio Rodríguez de Mendoza de Amazonas, Chachapoyas, 01001, Peru.

** Corresponding author. Center for Geospatial Research, Department of Geography, University of Georgia, Athens, GA 30602, USA.

E-mail addresses: elgar.barboza@untrm.edu.pe (E. Barboza), mmadden@uga.edu (M. Madden).

https://doi.org/10.1016/j.rsase.2026.102200
Received 30 August 2025; Received in revised form 28 July 2026; Accepted 6 August 2026
Available online 12 August 2026

and represents a replicable methodological contribution to agricultural monitoring and sustainable rural landscape management in similar contexts.

1. Introduction

Coffee (*Coffea arabica* L) is one of the world's most valuable agricultural commodities and one of the most widely consumed beverages, playing a fundamental role in the economy of many tropical countries (Torres et al., 2020). The coffee sector has experienced sustained growth across Africa, Asia, and the Americas, with particularly promising prospects in Latin America (Widjaya and Yanuarti, 2024). Peru is internationally recognized for producing high-quality Arabica coffee characterized by its distinctive aroma and flavor. Coffee is cultivated on more than 425,000 ha distributed across approximately 210 rural districts, providing livelihoods for more than 200,000 farming families (JNC, 2020; MINAGRI, 2018). Although the province of Chanchamayo (Junín) remains the country's principal producer, the departments of Amazonas and San Martín have substantially increased their production in recent years (JNC, 2020). Nevertheless, coffee production continues to face important challenges associated with market price fluctuations, pest outbreaks, diseases, and climate variability, which directly affect both cultivated area and producers' livelihoods (JNC, 2020; Julca-Otiniano et al., 2023).

Coffee cultivation is commonly established in heterogeneous tropical landscapes comprising forests, secondary vegetation, agricultural areas, and agroforestry systems. In these environments, shade-grown coffee frequently exhibits spectral characteristics similar to those of surrounding natural vegetation, making it difficult to discriminate using conventional optical remote sensing approaches. Furthermore, persistent cloud cover, rugged topography, and fragmented agricultural landscapes considerably reduce the accuracy and temporal consistency of Land Use and Land Cover (LULC) mapping in tropical mountain regions (Chemura et al., 2017; Kelley et al., 2018; Wachowiak et al., 2017). Consequently, reliable and up-to-date spatial information on coffee cultivation is essential for supporting sustainable agricultural management, environmental monitoring, certification processes, and territorial planning.

Recent advances in Earth observation have considerably improved the monitoring of agricultural systems. Sentinel-2 multispectral imagery provides detailed spectral information for vegetation characterization, whereas Sentinel-1 Synthetic Aperture Radar (SAR) supplies structural information independent of atmospheric conditions, allowing continuous observations in regions frequently affected by cloud cover (Marin et al., 2021; Maskell et al., 2021; Putra et al., 2020). Likewise, cloud computing platforms such as Google Earth Engine (GEE) have facilitated processing of large satellite image archives, while machine learning algorithms have substantially improved LULC classification performance (Gorelick et al., 2017). Several studies have successfully applied these technologies to map coffee cultivation and agroforestry systems in different countries. For example, Sentinel-2 imagery achieved an overall accuracy of 84% for coffee mapping in Nigeria (Hegazy and Kaloop, 2015), while the integration of deep learning and Sentinel-2 imagery produced classification accuracies close to 95% in Vietnam (Le et al., 2022). Likewise, the combination of Sentinel-1 and Sentinel-2 imagery improved crop discrimination in Morocco(Saad et al., 2022), mango mapping in Zimbabwe (Maskell et al., 2021), and agroforestry classification in Mexico (Escobar-López et al., 2022), demonstrating the advantages of integrating multisource remote sensing data.

Despite these advances, important methodological challenges remain. Most previous studies have focused on mapping coffee plantations or agroforestry systems independently, whereas relatively few have simultaneously produced detailed LULC classifications alongside coffee cultivation maps to better understand the landscape context surrounding coffee-growing areas. In addition, previous investigations have employed different combinations of optical imagery, radar data, machine learning algorithms, and validation strategies, making methodological comparisons difficult and limiting the identification of operational workflows applicable to tropical mountainous regions (Kelley et al., 2018; Maskell et al., 2021; Poortinga et al., 2019; Saad et al., 2022). Furthermore, studies integrating Sentinel-1 SAR, Sentinel-2 multispectral imagery, topographic variables, feature-selection procedures, and cloud-computing platforms remain scarce in Peru despite the country's importance as one of the leading Arabica coffee producers in South America (Medina et al., 2026).

To address these limitations, this study proposes an integrated methodology that combines Sentinel-1 SAR, Sentinel-2 multispectral imagery, topographic variables, feature selection using the Variance Inflation Factor (VIF), Random Forest (RF) classification, and cloud computing via GEE. Rather than introducing a new classification algorithm, the main contribution of this study lies in the integration of these complementary components into a reproducible framework for multitemporal mapping of coffee cultivation in tropical mountainous environments. Unlike previous investigations that focused exclusively on coffee plantation mapping, the proposed framework simultaneously generates annual LULC maps comprising eleven thematic classes, in which shade-grown and sun-grown coffee are explicitly represented as LULC classes. Binary coffee cultivation maps are subsequently derived from this LULC framework to facilitate the analysis of coffee distribution and temporal dynamics. This integrated approach provides a more comprehensive assessment of coffee cultivation and its relationship with the surrounding landscape under tropical mountain conditions.

Therefore, the objective of this study was to develop and evaluate an integrated methodology for mapping coffee cultivation using vegetation cover and LULC in the tropical region of Jaen and San Ignacio, Cajamarca (Peru), based on Sentinel-1 and Sentinel-2 data, machine learning, and GEE. Specifically, the study aimed to (i) evaluate the contribution of multisource remote sensing variables to improve LULC classification, (ii) generate annual maps of shade-grown coffee, sun-grown coffee, and the principal LULC classes between 2019 and 2024, and (iii) analyze the spatial distribution of coffee cultivation under different environmental conditions of elevation, slope, precipitation, and temperature.

2. Materials and methods

2.1. Study area

In northeastern Peru, we find the provinces of Jaen and San Ignacio, located in the northern part of the department of Cajamarca, with areas of 5232.57 km^2 and 4990.3 km^2, respectively (Fig. 1). Their altitudes range from 400 to 2800 m above sea level. They have a warm and humid climate, with average annual temperatures of 22 to 26 °C and rainfall between 813 and 1334 mm, providing ideal conditions for agricultural activities such as coffee cultivation (INEI, 2022). These provinces are home to a wide range of biodiversity, notably tropical and subtropical rainforests, as well as iconic species such as the spectacled bear (*Tremarctos ornatus*) and endemic birds such as the cock-of-the-rock, Peru's national bird (*Rupicola peruvianus*)(SENAMHI, 2020).

Coffee production is an agricultural activity in Jaen and San Ignacio, with annual yields of 30,000 and 25,000 tons/year, consolidating them as leaders in northern Peru. Coffee cultivation is mainly carried out under rainfed conditions in suitable agro-climatic conditions, providing the economic livelihood of local families and surpassing other crops such as rice and cocoa in importance (Ocaña-Zuñiga et al., 2025; SENAMHI, 2020).

The methodological process for mapping coffee cultivation in tropical ecosystems using Sentinel optical and radar data and a Random Forest model is shown in Fig. 2. The first step involved acquiring and preprocessing Sentinel-2, Sentinel-1, and topographic (digital elevation model) data. The preprocessing of the optical data consisted of masking clouds and cloud shadows, calculating spectral indices using Sentinel-2 bands, computing spatial-temporal metrics from Sentinel-1, and deriving slope and aspect. The results of the previous steps were used to create a layer stack and select the most essential variables using the Variance Inflation Factor (VIF) (O'brien, 2007). Finally, supervised classification and evaluation of the thematic accuracy of the final mapping were performed.

2.2. Data acquisition

Data acquisition was performed using the GEE platform (Gorelick et al., 2017; Tamiminia et al., 2020), which consisted of data from the Sentinel-1 (ID: COPERNICUS/SENTINEL-1_GRD) and Sentinel-2 (ID: COPERNICUS/SENTINEL-2_SR_HARMONIZED) collections, as well as topographic data (ID: USGS/SRTMGL1_003). The resolutions of the Sentinel-2 data ranged from 10 to 60 m (Table S1), the Ground Resolution Data (GRD) from Sentinel-1 C-band SAR was 10 m, and the digital elevation model from the Shuttle Radar Topographic Mission (SRTM) was 30 m. The time filter applied to Sentinel-1 and Sentinel-2 images was from December 1, 2018, to November 30, 2024, covering the wet and dry seasons (December to May) and the dry seasons (June to November) (Fig. S1). The result was a composite image (computed using the median) for each season and year. This definition was based on historical time series analysis.

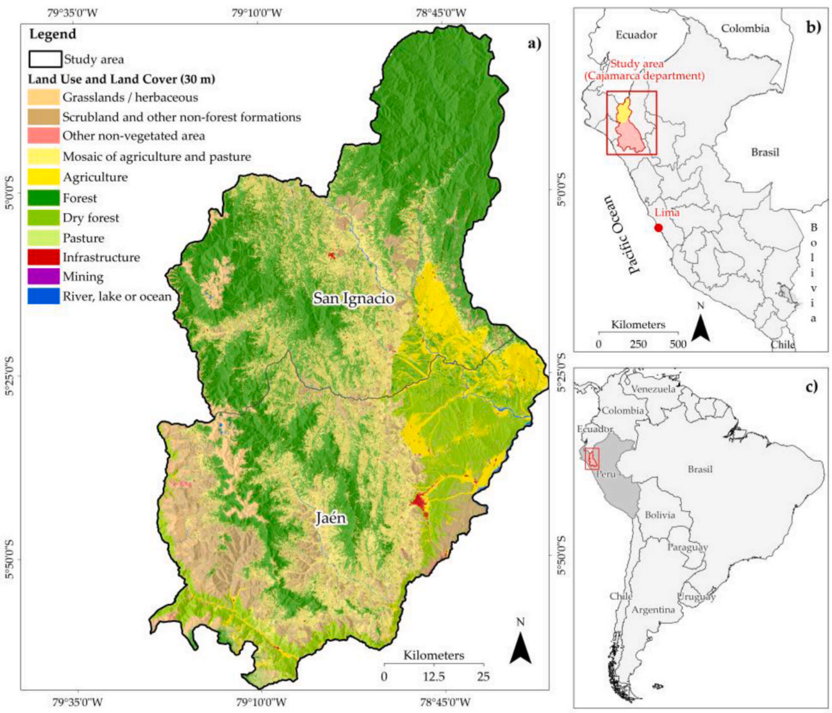

Fig. 1. Location of the study area: a) provinces of Jaen and San Ignacio, b) department of Cajamarca, and c) Peru in South America.

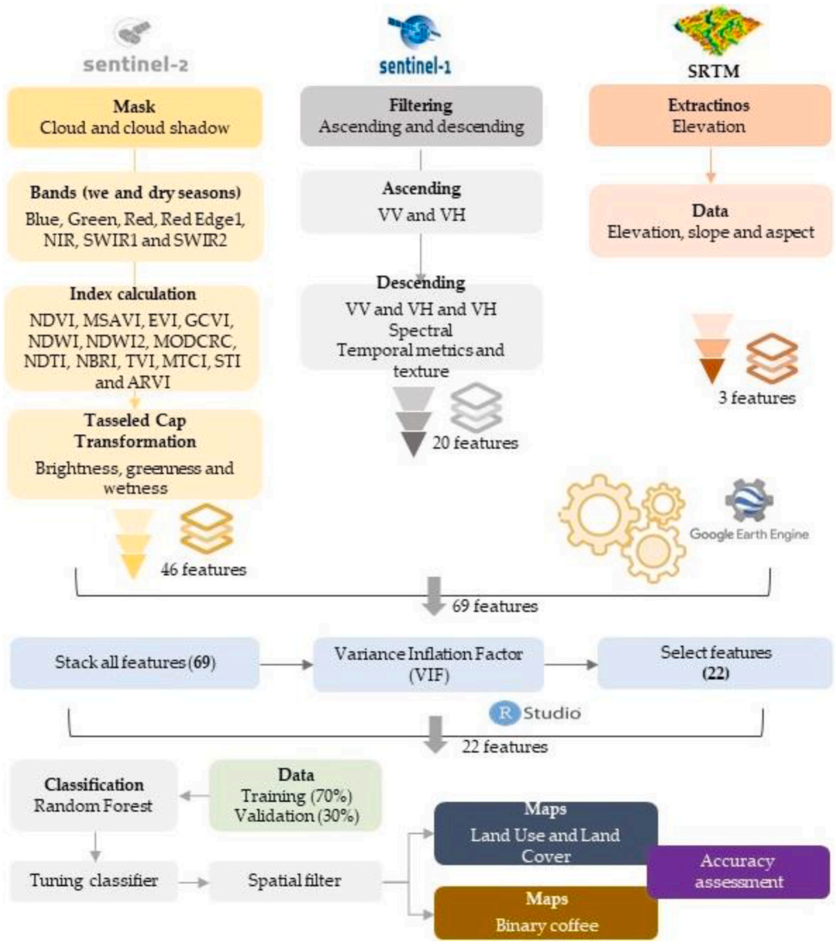

Fig. 2. Methodological process for mapping coffee using Sentinel and GEE data in tropical ecosystems in Peru.

Images with < 30% cloud cover were considered, followed by cloud masking using the cloud score algorithm implemented in GEE and the Temporal Dark Outlier Mask (TDOM) method (Barboza et al., 2020; Housman et al., 2018; Schmitt et al., 2019) for each mosaic per season and per year. TDOM improves cloud shadow detection by obtaining a dark pixel anomaly as clouds move (Nguyen et al., 2020). Vertical-vertical (VV) and vertical-horizontal (VH) polarizations were used for Sentinel-1. Topographic data were obtained from SRTM with a resolution of 30 m (Farr et al., 2007).

2.3. Preprocessing of spatial data

The Sentinel-2 image collection was subdivided into wet and dry seasons for each year from 2019 to 2024. The mosaic for each annual season was calculated using the median, where maximum or minimum values could be contaminated by clouds and cloud shadows (Maskell et al., 2021). Spectral indices were calculated for each mosaic using band mathematics with the Tasseled Cap Transformation (Shi and Xu, 2019), which were included as individual bands in each scene (Table S2). These metrics have been used for optical images, such as Landsat, in less cloudy regions (Hu et al., 2018; Müller et al., 2015).

Following the proposal by Maskell et al. (2021), temporal statistics derived from SAR and texture characteristics were calculated for both polarizations (VV and VH) for the Sentinel-1 scenes (Table S3). For this process, spectral temporal statistics were first calculated for the descending VV and descending VH time series, including the median, 25th and 75th percentiles, and standard deviation for each scene (Table S3). Based on the above result, spectral temporal metrics were determined using eight texture variables from the Gray Level Co-occurrence Matrix (GLCM) as reported in different studies (Drielsma et al., 2022; Haralick et al., 1973; Lelong and Thong-Chane, 2003; Moreira and Valeriano, 2014). Likewise, for the median composite of the descending VH series using a 5×5 moving window, with a displacement of 1, and averaged in four spatial orientations (Maskell et al., 2021). This is because SAR Sentinel-1 texture information has been shown to help discriminate land cover types and land use in heterogeneous coffee plantation landscapes, mapping agroforestry systems, and distributing disturbances in tropical forests (Balling et al., 2023; Kawakubo and Pérez Machado, 2016; Mishra et al., 2019; Numbisi et al., 2019).

$$VIF = \frac{1}{1 - R^2} \quad (1)$$

All layers derived from the Sentinel-2 and Sentinel-1 collections, as well as topographic variables (elevation, slope, and aspect), were cropped within the study area and combined into a single multiband image, resulting in a collection of 69 bands with a resolution of 10 m (Tables S2 and S3), as a result of the resampling applied in GEE. It has been shown that many input bands can be highly correlated with each other, which can negatively affect the detection and classification of minority classes during model application (Hasanuzzaman et al., 2024; Waldner et al., 2019). To avoid multicollinearity between bands, a VIF was applied (Dormann et al., 2013; O'brien, 2007).

The characteristics obtained through sampling at the reference points were exported from GEE and analyzed in R Studio. VIF was determined using Equation (1), where R^2 is the coefficient of determination, calculated for each band. Any feature with a VIF greater than 10 was removed. Although VIF reduced the predictor set from 69 to 22 variables, the selected subset maintained the main biophysical characteristics associated with coffee cultivation. The retained variables included vegetation indices related to canopy vigor and moisture, SAR backscatter metrics describing vegetation structure, texture variables representing canopy heterogeneity, and topographic variables controlling local environmental conditions. Therefore, the reduction primarily removed redundant information rather than agronomically relevant predictors (Table 1 and Fig. S2).

We applied a sensitivity analysis performed on 648 combinations of hyperparameters of the RF algorithm (Breiman, 2001) to evaluate the model's performance using the Kappa coefficient based on the values of n_trees, var_split, and bag_fraction. This will allow us to determine the appropriate parameters for classifying LULC maps.

2.4. Classification of LULC maps

The reference data for parameterizing, training, and validating the classification were collected using high-resolution images such as Google Earth and Planet Scope for 2019, 2020, 2021, 2022, 2023, and 2024 across the entire study area. Field data were also collected during the 2023 dry season, where the Locus Map app's location points for the different LULC classes were georeferenced (Barboza et al., 2024). We used a classification scheme for both data sets with examples of high-resolution images from Google Earth for the reference data (points/pixels). If the randomly sampled data fell between classes or in a mixed area, it was resampled within the training area previously defined in GEE for all relevant courses. Likewise, iterative sampling was applied for coffee and cultivated vegetation classes, as these classes are most often confused with coffee. The reference samples were randomly divided into training (70%) and validation (30%) datasets using stratified random sampling to preserve the proportional representation of each LULC class. A fixed random seed was adopted to ensure reproducibility of the sampling process. The same sampling strategy was independently applied for each annual classification. A total of ~35,000 points per year were determined, ensuring that each class had at least 3000 training points (Fig. 3).

To eliminate salt and pepper classification errors, a spatial filter based on the GEE "connectedPixelCount" function was applied to each year's LULC maps (Crawford et al., 2013). Fill filters were also applied to replace information gaps caused by clouds with consistent temporal classification values, and a temporal filter was used to identify class transitions following the methodology proposed by Turpo et al. (2022). A minimum mappable area of approximately 0.5 ha was considered.

Table 1
Features entered the classifier after feature reduction (using a VIF method).

Category	Features included (22)
Sentinel-2- dry season	GCVI
	MSAVI
	NDWI
	Blue
	NIR
	Red Edge 1
Sentinel-2- wet season	NIR
	EVI
	STI
	NDWI
Sentinel-1 SAR (including spatiotemporal metrics)	VV_a
	VV_d_sd
	VV_d_75
	ratio_VH_VV_a
	ratio_VH_VV_d
Sentinel-1 SAR texture metrics	VH_d_corr
	VH_d_contrast
	VH_d_svar
	VH_d_asm
Metrics derived from the DEM	Elevation
	Slope
	Aspect

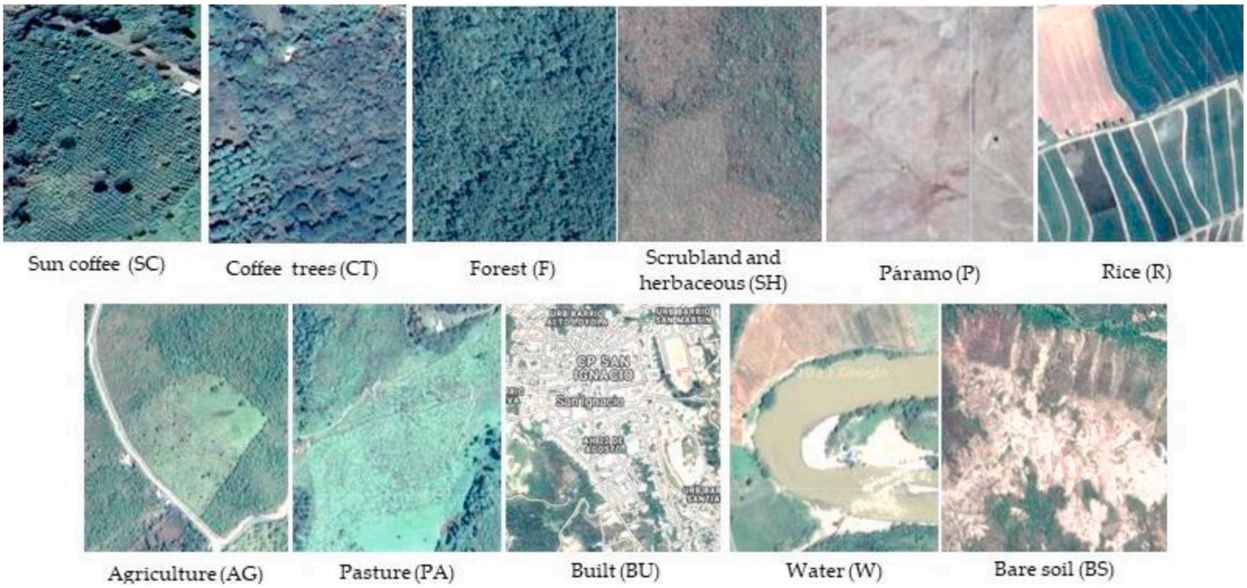

Fig. 3. Classification scheme, with examples of high-resolution images from Google Earth for reference data (points/pixels).

2.5. *Thematic validation*

The accuracy of the LULC classification was evaluated using a cross-validation analysis employing a confusion matrix, constructed from reference data (actual classes) and data predicted by the model for each year of study. From this matrix, the following metrics were calculated: Overall Accuracy (OA), Kappa index (κ), Producer precision (Recall), User's precision (Accuracy), F1-Score, Omission error, and Commission error. These metrics were calculated for each class and year, allowing for the evaluation of the temporal performance and stability of the classification model.

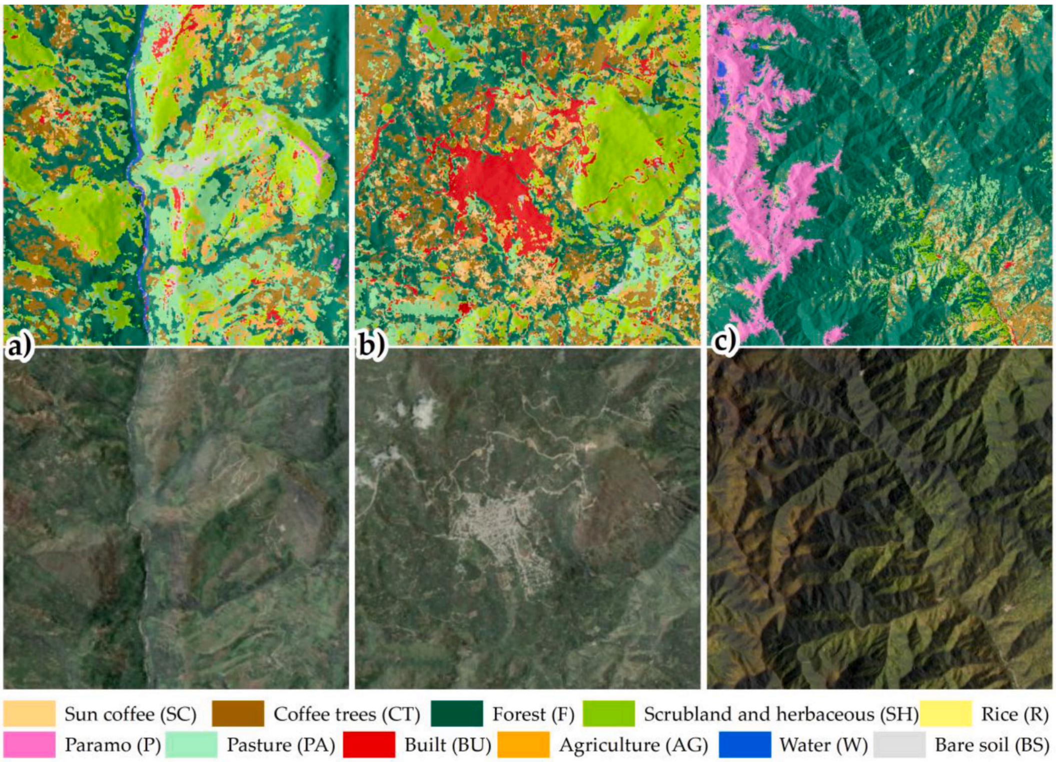

Fig. 4. The study includes the types of land use and land cover.

2.6. LULC changes and spatial and environmental patterns of coffee cultivation

The LULC maps were analyzed in two periods: 2019–2021 and 2021–2024, to identify changes, continuities, and transitions between classes. At the same time, the spatial and environmental patterns associated with coffee cultivation were evaluated, integrating the cultivated areas by combining the classes corresponding to all the years of the study (2019–2024). These areas were superimposed on environmental layers available in GEE, including slope and elevation (USGS/SRTMGL1_003), annual precipitation (UDEL/PETM/ANNUAL), and average yearly temperature (WORLDCLIM/V1/BIO). For each coffee polygon, the values associated with each variable were extracted, reclassified, and spatially analyzed. This approach made it possible to identify the optimal topographic and climatic conditions that define the ecological niche of coffee in the study region.

3. Results

3.1. Multitemporal vegetation cover maps

The results for determining the hyperparameters for classifying coffee crops and LULC in the study area showed that the Kappa value remained constant (0.84) for a wide range of combinations, particularly when n_trees was set to 400 and bag_fraction to 0.9. When comparing the var_split values, it was evident that configurations such as var_split = 1 and var_split = 3 offered the same performance. The integration of Sentinel-1, Sentinel-2, and topographic data allowed for a detailed classification of the 11 LULC classes, covering an area of approximately 10,222.87 km^2. The classes were sun coffee (plots with only coffee plants) (SC), coffee trees (plots with coffee plants and other forest species) (CT), forest (F), scrubland and herbaceous (SH), Paramo (P), rice (R), agriculture (AG), Pasture (PA), built (BU), water (W), and bare soil (BS) (Fig. 4). The classified and natural-color cultivation of unshaded and shaded coffee is shown in Fig. 4a–b, while the paramo, pastures, and forests classes are presented in Fig. 4c.

In the province of San Ignacio, changes in LULC between 2019 and 2024 show spatial stability with slight interannual variations. Forest cover remained the dominant class, with values ranging from 3240.13 km^2 in 2019 to 3268.63 km^2 in 2024, totaling 19,670.93 km^2 in the period analyzed. Coffee plantations, grouped into the SC and CT classes, occupied 1691.27 km^2, with CT being more extensive, reaching 298.97 km^2 in 2020 as its peak. Pasture areas also showed a significant presence with a cumulative 3000.66 km^2, although with a slight reduction in recent years, from 541.42 km^2 in 2020 to 421.96 km^2 in 2024. On the other hand, scrub and herbaceous areas grew significantly, from 388.37 km^2 in 2022 to 555.31 km^2 in 2024, which could be related to agricultural abandonment or secondary regeneration processes.

Similar patterns were observed in the province of Jaen, with more marked variations. Forest cover was also dominant, increasing from 1772.72 km^2 in 2019 to 1891.37 km^2 in 2024, for 10,870.59 km^2. However, scrubland and grassland areas had a much greater weight than San Ignacio, with a total of 7539.98 km^2, surpassing coffee plantations and agricultural land. The area dedicated to rice remained high and stable, totaling 1267.77 km^2, peaking in 2020 with 219.50 km^2. Areas of bare soil reached 3778.71 km^2 over the entire period, with a peak of 680.25 km^2 in 2020, which contrasts sharply with San Ignacio. Finally, urbanized areas also grew slightly, from 75.13 km^2 in 2019 to 103.65 km^2 in 2024, possibly reflecting processes of urban expansion and land use change (Table 2).

SC and CT are distributed in the study area from north to south between the districts of San José de Lourdes, San Ignacio, Huarango,

Table 2
Area (km^2) of LULC classes for the provinces of San Ignacio and Jaen.

LULC	2019	2020	2021	2022	2023	2024
San Ignacio						
Sun coffee (SC)	25.56	26.77	14.04	31.80	31.48	23.50
Coffee trees (CT)	261.88	298.97	285.38	294.16	273.26	277.61
Forest (F)	3240.13	3245.34	3387.23	3288.72	3240.88	3268.63
Scrubland and herbaceous (SH)	465.94	406.85	392.59	388.37	477.45	555.31
Paramo (P)	99.00	90.91	94.50	89.61	79.60	85.70
Rice (R)	34.61	30.23	32.11	31.53	40.84	37.15
Agriculture (AG)	127.69	148.02	128.58	157.84	147.35	112.30
Pasture (PA)	531.04	541.42	461.42	529.17	515.66	421.96
Built (BU)	69.56	67.76	73.21	69.05	72.54	80.05
Water (W)	10.94	13.17	12.36	14.35	12.49	11.36
Bare soil (BS)	44.02	40.94	28.96	15.76	18.81	36.81
Jaen						
Sun coffee (SC)	50.06	60.53	43.63	41.54	49.73	42.55
Coffee trees (CT)	199.20	187.98	188.61	169.99	161.42	175.79
Forest (F)	1772.72	1818.52	1886.55	1754.91	1746.52	1891.37
Scrubland and herbaceous (SH)	1248.96	1192.12	1286.43	1344.56	1266.11	1201.80
Paramo (P)	162.98	154.80	156.82	160.84	143.09	190.10
Rice (R)	211.88	219.50	215.93	213.72	207.79	198.94
Agriculture (AG)	450.72	435.09	422.81	478.19	506.83	449.32
Pasture (PA)	195.13	178.46	145.12	173.41	173.74	149.67
Built (BU)	75.13	87.87	90.40	93.98	103.80	103.65
Water (W)	22.49	23.66	21.58	20.09	16.47	18.32
Bare soil (BS)	649.48	680.25	580.91	587.54	663.26	617.26

Chirinos, Santa Rosa, La Coipa, Tabaconas, San José del Alto, Huabal, Las Pirias, Chontali, and Colasay (Fig. 5). The forest type is located in the highest altitude areas of both provinces, between the northeast and southwest of San Ignacio. In contrast, the province of Jaen is situated in the center and northwest. Agricultural areas, where rice is grown, are located near bodies of water (the Marañón, Amojú, and Chichipe rivers) and urban areas, mainly in the provincial and district capitals (e.g., Jaen and San Ignacio). Areas without vegetation or bare land are located in the south and southwest of the province of Jaen, mainly represented by bare sandbanks.

3.2. Cartographic accuracy

The accuracy for the user (i.e., commission error) of the generated maps shows consistently high values, exceeding 95% in most classes and years, indicating high reliability in label assignment and low commission error. However, the CT and PA classes show slight variability in some years (Fig. 6a), which could reflect confusion with neighboring coverages such as AG and SH (Fig. 6b). On the other hand, the omission error shows that SC and CT have the highest values, particularly in 2019, 2022, and 2024, with omissions exceeding 10% in some cases (Fig. 6c), suggesting a lower sensitivity of the model to detect these classes in those periods.

The commission error was generally low for all classes (<5%), confirming the accuracy of the models in class assignment (Fig. 6d). However, slight increases were observed in the CT class in some years. Overall, the F1-Score performance remained high in most classes (>0.90), indicating a good balance between the model's precision and sensitivity (Fig. 6e). Finally, the OA ranged from 0.84 (2019) to 0.91 (2022 and 2024), while the Kappa index varied between 0.82 and 0.90 (Fig. 6f), reflecting acceptable performance and substantial agreement between the classified maps and the reference data.

3.3. Binary map coffee/no coffee

The area under coffee cultivation in the provinces of Jaen and San Ignacio during the period 2019-2024 shows variations with reductions and increases in some years (Fig. 7). In the province of Jaen, the area under coffee cultivation was 249.27 km^2 in 2019, with a slight decrease in the following years, reaching 211.15 km^2 in 2023. However, in 2024, there was an increase, with a cultivated area of 218.34 km^2. On the other hand, the province of San Ignacio showed a different trend, with an increase in the area under coffee cultivation from 287.44 km^2 in 2019 to 325.97 km^2 in 2022, with a slight decrease in 2023 (304.74 km^2) and stability in 2024 (301.12 km^2).

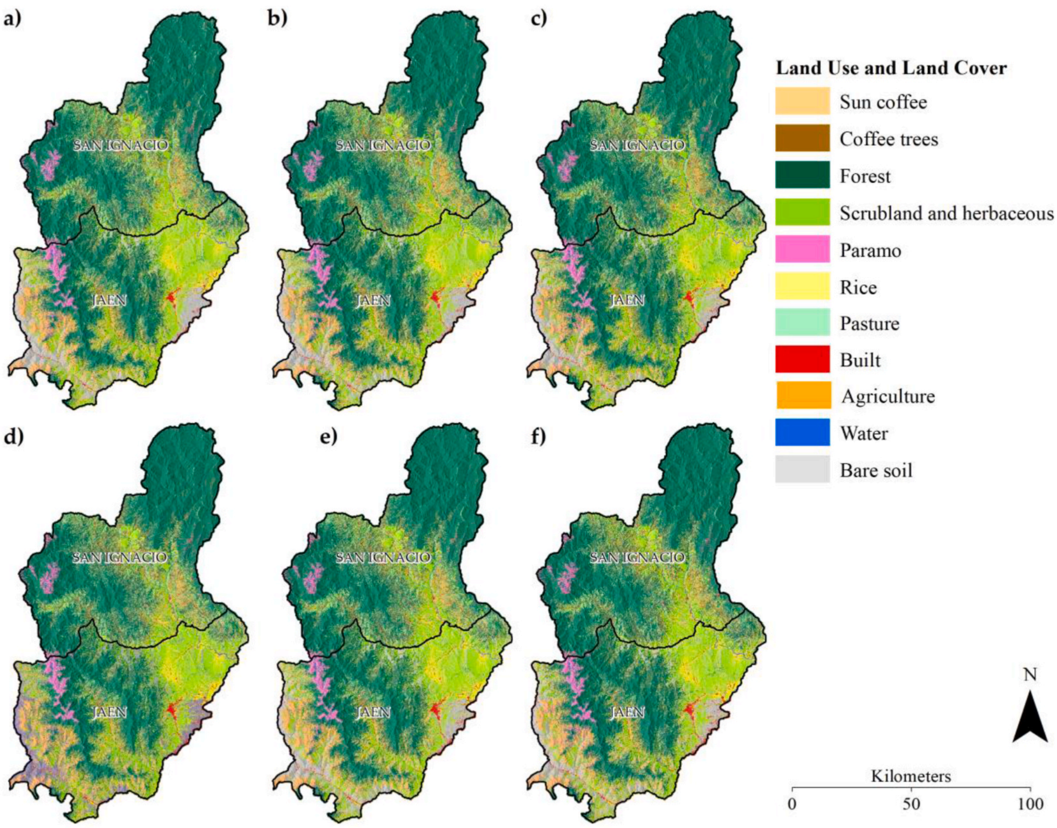

Fig. 5. Land use and land cover in study area for years a) 2019, b) 2020, c) 2021, d) 2022, e) 2023 and f) 2024.

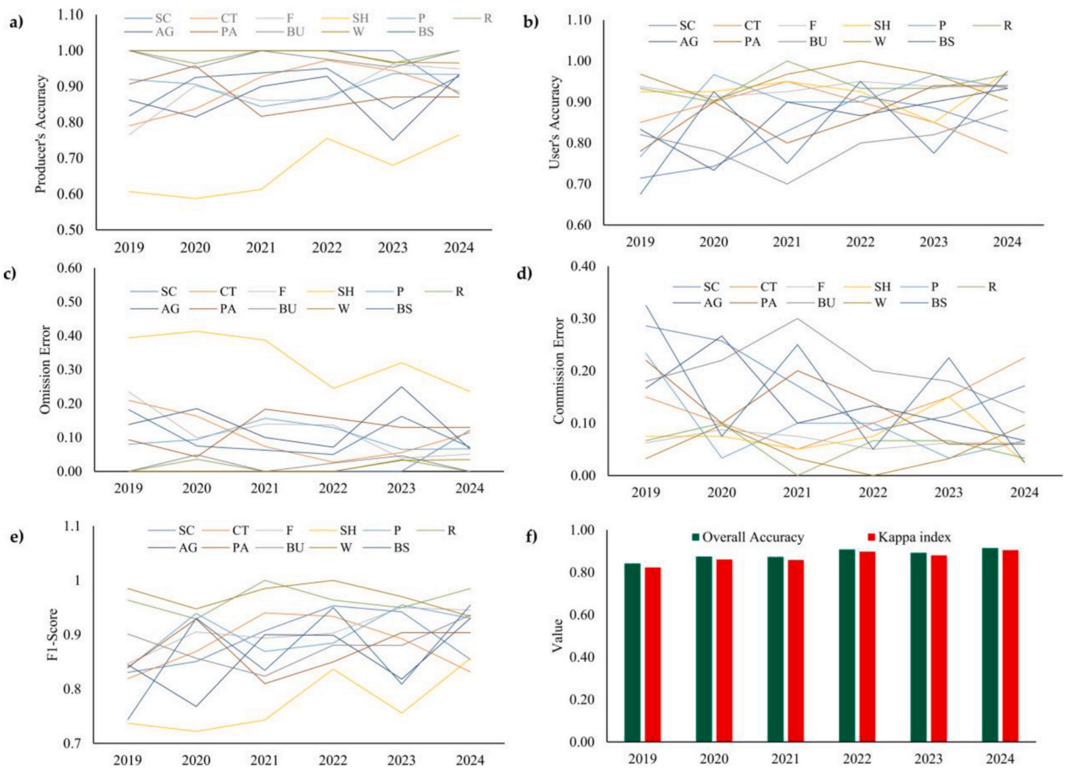

Fig. 6. Accuracy metrics for maps generated from coffee mapping: a) Producer's Accuracy, b) User's Accuracy, c) Omission Error, d) Commission Error, e) F1-Score, and f) Overall Accuracy and Kappa index.

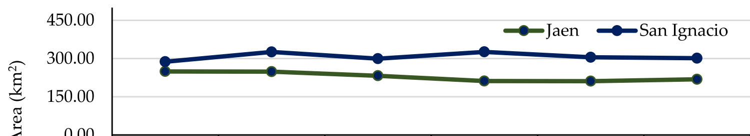

	2019	2020	2021	2022	2023	2024
Jaen	249.27	248.51	232.24	211.53	211.15	218.34
San Ignacio	287.44	325.73	299.42	325.97	304.74	301.12

Fig. 7. Coffee cultivation area for the provinces of Jaen and San Ignacio.

Fig. 8 shows the spatial distribution of coffee cultivation by province. The area cultivated with sun and trees coffee extends from the center of the province of Jaen to the east, north, and west of San Ignacio.

3.4. Land use and land cover change dynamics

In the first period (P1, 2019–2021), the greatest loss occurred in the sun coffee class (68.26%), followed by pasture (49.03%) and coffee trees (38.59%). The most significant gains were recorded in sun coffee (44.52%), coffee trees (41.39%), and built-up areas (40.62%). The highest net positive changes corresponded to sun coffee (−23.74%) and built-up areas (13.08%) (Fig. 9a).

In the second period (P2, 2021–2024), the sun coffee class again showed the largest loss (64.77%), followed by pasture (52.01%) and coffee trees (45.37%). The highest gains were observed in sun coffee (79.30%), pasture (46.25%), and agriculture (44.98%). Net positive changes were most notable for sun coffee (14.53%) and agriculture (1.86%) (Fig. 9b).

The distribution of coffee cultivation according to topographical and climatological variables is shown in Fig. 10. Coffee-growing areas are between 0 and 50%, indicating a preference for moderately sloping terrain (Fig. 10a). About altitude (Fig. 10b), the crop is grown at altitudes ranging from 500 to 2500 m above sea level, which coincides with the optimal conditions for Arabica coffee in mountainous areas.

In terms of precipitation (Fig. 10c), coffee plantations are distributed in the regions that receive between 400 and 1000 mm of annual rainfall, while in terms of average yearly temperature (Fig. 10d), coffee is mainly found in areas with temperatures between 15 and 24 °C, which are favorable climatic conditions for its growth and phenological development.

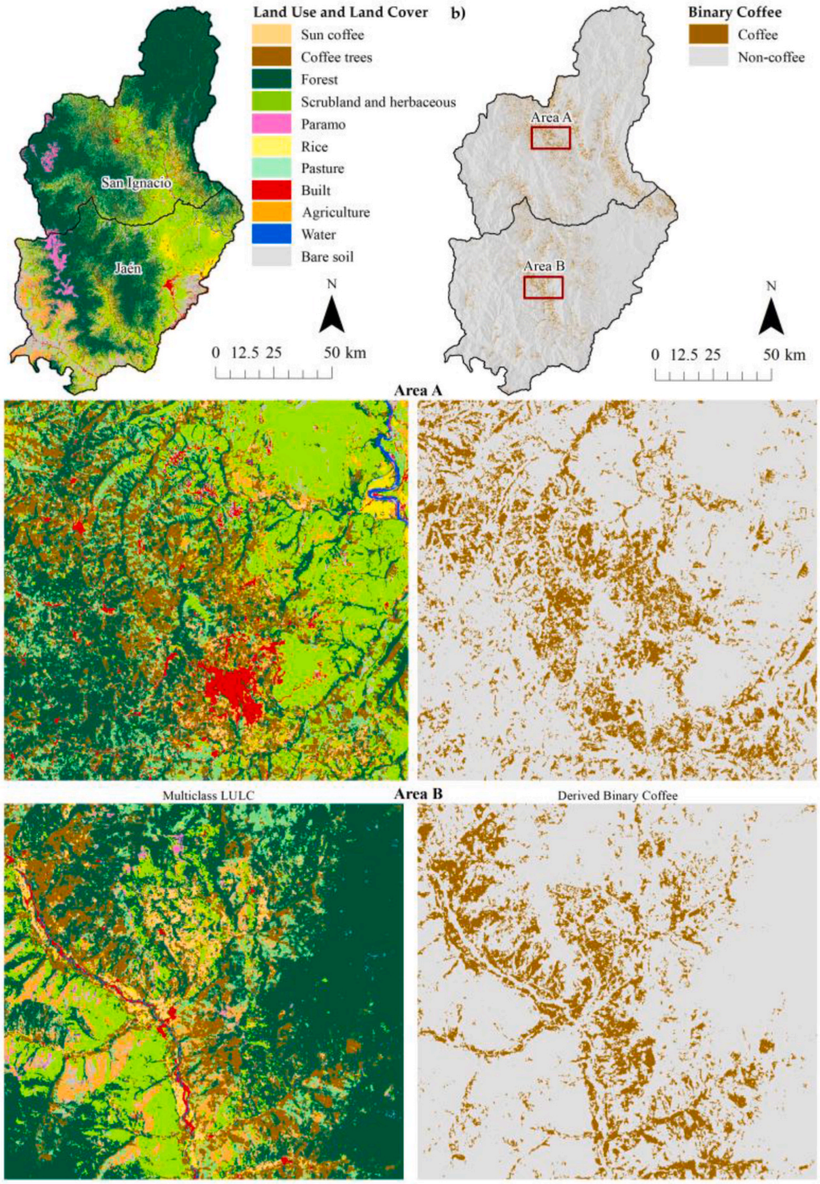

Fig. 8. Comparison between the a) multiclass LULC classification and the b) derived binary coffee map. Areas A and B show representative subregions illustrating how the shade-grown and sun-grown coffee classes from the LULC classification are integrated into a binary coffee/non-coffee product.

4. Discussion

In this study, we mapped coffee crops using an LULC classification framework based on Sentinel data and machine learning techniques in tropical ecosystems in Cajamarca, Peru, to identify coffee-growing areas and types of vegetation cover and land use. This is one of the first attempts to map coffee crops in tropical ecosystems in Peru. In this study, we focused on large-scale mapping of a permanent crop, following the methodology of Maskell et al. (2021), who integrated Sentinel optical and radar data to map smallholder coffee production systems in Vietnam. Unlike previous studies that primarily focused on coffee plantation mapping as a single classification target, our workflow simultaneously generated multitemporal LULC maps and coffee-specific maps derived from the same classification framework. This unified approach enables a more comprehensive assessment of coffee cultivation dynamics while preserving the spatial context of the surrounding landscape, representing one of the main methodological contributions of this study.

The methodology presented is based on the use of open data and its processing on freely accessible platforms such as GEE and R Studio for mapping coffee cultivation in heterogeneous areas that are very complex to map due to the characteristics of the landscapes.

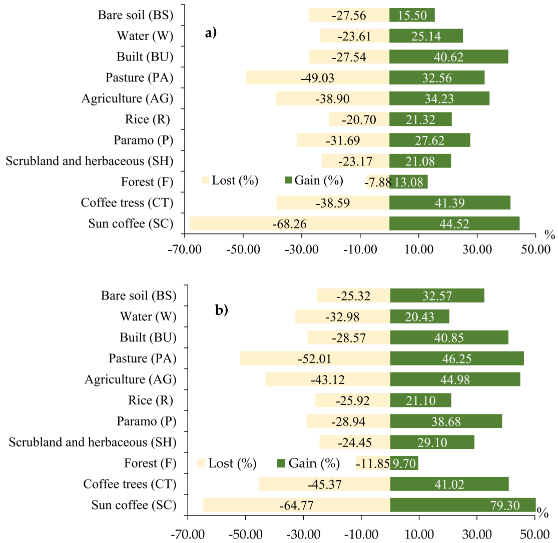

Fig. 9. Gain and loss by class and period of analysis in the study area, a) 2019-2021 and b) 2021-2024.

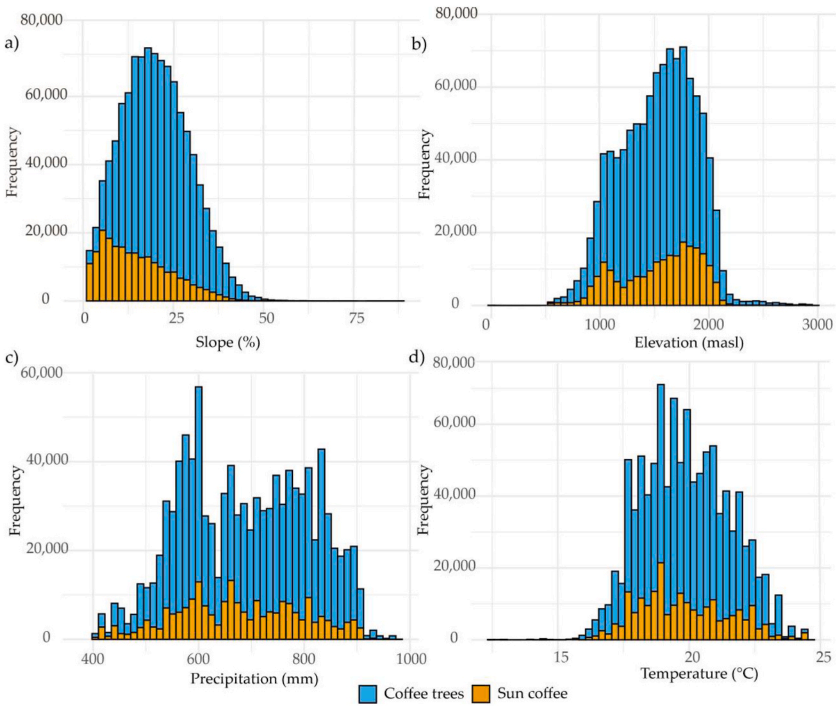

Fig. 10. Spatial patterns of slope (a), elevation (b), annual precipitation (c), and temperature (d) of coffee in the study area.

Many studies have used Sentinel data for large-scale crop mapping, generally focusing on crops such as corn, cotton, rice, sorghum, soybeans, and wheat (Adrah et al., 2025; Aires et al., 2025; Liu et al., 2025; Medina Medina et al., 2024; Qiu et al., 2025; Zhao et al., 2024). Rather than proposing a new classification algorithm, the main contribution of this work lies in the integration of multisource remote sensing data, feature selection, machine learning, and cloud computing into a reproducible workflow for coffee cultivation mapping in tropical mountainous environments.

The optical remote sensing data, such as that from many NASA satellites, has several limitations that affect its usefulness for detailed ground analysis. The spatial resolution is often too coarse to capture fine-scale features, making it difficult to monitor small land cover changes. Additionally, the spectral resolution may be insufficient to distinguish between similar vegetation types or subtle surface variations. Optical sensors also cannot penetrate cloud cover or smoke, which can result in data gaps or reduced reliability, especially in regions with frequent atmospheric interference. Furthermore, these sensors are unable to penetrate dense forest canopies, limiting visibility of ground-level or understory conditions. In recent years, the integration of Sentinel-1 and Sentinel-2 data in crop mapping has been widely applied in different parts of the world, allowing for better crop classification and monitoring (Bahrami et al., 2022).

Including Sentinel-1 has the main advantage of overcoming cloud cover in areas with constant rainfall, as in the study area (Maskell et al., 2021). There are an increasing number of studies that integrate these two types of data in the mapping of forest plantations (Balling et al., 2023; Hu et al., 2018; Liu et al., 2018; Numbisi et al., 2019), crops (Mansaray et al., 2020; Qiu et al., 2022; W. F. Silva et al., 2009), and individual trees (Camino et al., 2025; Klehr et al., 2025; X. Liu et al., 2023; Schulz et al., 2024). At the level of mapping coffee production systems, studies have been developed in other areas such as Indonesia, Ethiopia, Vietnam, El Salvador, and Brazil, integrating Sentinel-1 and Sentinel-2 data and obtaining accuracies greater than 84% (Chemura et al., 2018; Kawakubo and Pérez, 2016; Le et al., 2022; Masolele et al., 2022; Ortega-Huerta et al., 2012; Son et al., 2023; Tridawati et al., 2020). In the present study, the additional incorporation of topographic variables complemented the spectral and structural information provided by Sentinel-2 and Sentinel-1, respectively. This multisource integration proved particularly valuable under the persistent cloud cover and complex topographic conditions of the Peruvian tropical Andes, improving the discrimination of coffee cultivation from surrounding LULC classes while maintaining consistent multitemporal observations.

The selection of variables in this study was based on biophysical and spectral criteria that explain the agronomic behavior of coffee crops under different management conditions (with or without shade). The spectral bands from Sentinel-2 allowed the calculation of vegetation indices such as NDVI, EVI, GCVI, MSAVI, and NDWI, which capture key aspects such as vegetation vigor, chlorophyll presence, active green cover, canopy moisture, and the effect of exposed soil (Bernardes et al., 2012; da Silva et al., 2024; Nogueira et al., 2018). These indices were fundamental in differentiating densely covered plots (trees whit coffee) from those that were more exposed (sun coffee), especially in the dry season, when the spectral response of the vegetation is more contrasting. On the other hand, metrics derived from Sentinel-1, such as VV, VH polarization, and their combinations, provided structural information about the crop, helpful in detecting differences in roughness, coverage density, and surface moisture, which are relevant attributes in cloudy conditions or where optical signals are limited (Haralick et al., 1973; Lelong and Thong-Chane, 2003; Silva et al., 2009).

In this context, coffee under shade trees generally presents greater surface roughness due to the heterogeneous canopy formed by multiple vegetation strata, higher coverage density because of overlapping foliage from trees and coffee plants, and greater surface moisture retention owing to reduced direct solar radiation and lower evapotranspiration rates (Avelino et al., 2023; Maskell et al., 2021; Somarriba et al., 2024). Conversely, sun coffee plots tend to exhibit smoother surface textures with more homogeneous canopy structure, lower overall coverage density, and reduced surface moisture, as the absence of shade increases soil exposure, accelerates drying, and leads to more uniform but less dense vegetation patterns (Ehrenbergerová et al., 2021). These structural contrasts explain the distinct backscatter responses in VV and VH polarizations and their derived ratios, which enhance the discrimination trees coffee and sun coffee systems in radar imagery (Bousbih et al., 2017; Bouvet et al., 2018).

Likewise, texture metrics derived from both optical and radar images provided a more detailed spatial characterization of the crop pattern, being particularly useful for identifying agroforestry systems with coffee with greater structural heterogeneity (Chemura et al., 2018; Le et al., 2022; Mansaray et al., 2020). For their part, topographic variables such as elevation, slope, and aspect, derived from the digital elevation model, allowed for the integration of the physical component of the landscape, given that coffee grows in specific altitudinal ranges and its productivity is influenced by sun exposure and terrain slope (Fekadu and Andarege, 2025; Liu et al., 2025; Salas et al., 2020; Tassew et al., 2021). Together, the combination of these variables strengthens the discriminatory capacity of the classification models and technically supports the detailed mapping of coffee in the study area.

The application of the Random Forest algorithm for supervised classification proved adequate due to its ability to handle complex, multicollinear datasets with noise, characteristics that are common in tropical mountainous environments. The evaluation of hyperparameters, which not only ensured stability in the results but also reduced the computational load without compromising accuracy. On the other hand, the LULC maps generated at a spatial resolution of 10 m allowed us to distinguish 11 classes of agricultural and natural landscape, including shade-grown coffee, non-shade-grown coffee, forest, agriculture, rice, grasslands, shrublands/grasslands, paramo, water bodies, urban areas, and bare soil, which could be important for developing projects or activities focused on a specific LULC class in the study area. The validation metrics were similar to those obtained in other studies (Escobar-López et al., 2022; Ibrahim et al., 2021; Le et al., 2022; Ortega-Huerta et al., 2012).

At the territorial level, there was evidence of spatial differentiation in the dynamics of coffee cultivation. In San Ignacio, the area under coffee cultivation experienced an upward trend between 2019 and 2022, stabilizing in 2024, which could be associated with local coffee promotion policies, the adoption of agroforestry systems, or productive reconversion processes. In Jaen, on the other hand, there was a slight contraction in the area under cultivation, followed by a partial recovery in the last year, possibly linked to market fluctuations, territorial restrictions, or technical limitations on crop expansion. These patterns were captured using binary coffee maps (coffee/non-coffee), a valuable tool for monitoring cultivated areas and territorial planning.

However, this study has some limitations. First, the lack of specific phenological and agronomic data (e.g., the age of the coffee trees, the varieties grown, canopy management, or fertilization) limits the model's ability to distinguish between productive subclasses or stages of crop development. Second, the low representativeness of certain classes and the high heterogeneity of land cover types such as grasslands and scrublands may have contributed to the errors observed in some classification metrics. Third, the training and validation samples were selected randomly; spatial dependence may exist between nearby observations. Consequently, the reported accuracy values should be interpreted as estimates of classification performance under the sampling design adopted in this study, rather than as absolute measures of the model's generalization. Furthermore, the absence of an independent external test dataset limits the assessment of the model's transferability beyond the study area. Furthermore, the propagation of uncertainty was not evaluated, which should be considered in future studies. Based on these results, developing a classification architecture based on deep learning models (e.g., CNN, U-Net) that can take advantage of spatial and temporal information more efficiently is proposed as a future line of research. Similarly, integrating socioeconomic information, land management data, and climatic variables would enrich the analysis and link the generated cartography with real productive processes and adaptation strategies to climate change.

In this sense, the proposed approach constitutes a first methodological step for the systematic and multiannual monitoring of coffee in tropical Andean-Amazon regions. Furthermore, it lays the foundations for developing automated geographic information systems oriented towards sustainable management of the rural landscape, agricultural planning, and decision-making in public policies related to the coffee sector. The methodology applied in this study still needs to be demonstrated in other coffee-growing regions. Future studies could integrate other classification methods, such as neural networks, using multispectral images from drones as training areas to classify high and medium-resolution images, and incorporating metrics obtained from LiDAR data and cross-validation to improve crop classification accuracy.

5. Conclusions

This study developed an integrated methodology for mapping coffee cultivation based on vegetation LULC in the tropical region of Jaen and San Ignacio, Cajamarca (Peru), by integrating Sentinel-1 SAR, Sentinel-2 multispectral imagery, topographic variables, RF classification, and GEE. The proposed approach achieved overall accuracies above 84% and Kappa coefficients between 0.82 and 0.90, demonstrating its capability to discriminate shade-grown coffee, sun-grown coffee, and the principal LULC classes under the environmental conditions of the study area. Feature selection reduced the predictor set from 69 to 22 variables, highlighting the importance of combining spectral indices, SAR metrics, texture measures, and topographic variables to improve classification performance.

The multitemporal maps revealed changes in coffee cultivation between 2019 and 2024 and showed that coffee distribution was mainly associated with specific ranges of elevation, slope, precipitation, and temperature. From a practical perspective, the obtained classification accuracy provides a reliable basis for regional-scale monitoring of coffee cultivation, supporting agricultural planning, land-use change assessment, and environmental management in the study area. Although the methodology showed operational performance in northern Cajamarca, its potential applicability to other coffee-producing regions or agroforestry systems should be evaluated in future studies before broader generalization.

CRediT authorship contribution statement

Elgar Barboza: Conceptualization, Data curation, Formal analysis, Funding acquisition, Investigation, Methodology, Software, Visualization, Writing – original draft, Writing – review & editing. **Amanda Aragon:** Conceptualization, Investigation, Methodology, Supervision, Writing – review & editing. **Samuel Pizarro:** Investigation, Methodology, Software, Visualization. **Alcides Roman:** Investigation, Validation, Writing – original draft. **Brandon Adams:** Investigation, Methodology, Software, Supervision. **Ellen Delgado:** Investigation, Methodology, Visualization, Writing – review & editing. **Alexander Cotrina-Sanchez:** Investigation, Visualization, Writing – review & editing. **Aqil Tariq:** Investigation, Methodology, Writing – review & editing. **Angel J. Medina-Medina:** Investigation, Methodology, Visualization, Writing – review & editing. **Katerin M. Tuesta-Trauco:** Investigation, Methodology, Visualization, Writing – review & editing. **Abner S. Rivera-Fernandez:** Investigation, Methodology, Visualization, Writing – review & editing. **Jhon A. Zabaleta-Santisteban:** Investigation, Methodology, Validation, Visualization, Writing – review & editing. **Candy Ocaña:** Conceptualization, Investigation, Methodology, Supervision, Validation, Visualization, Writing – review & editing. **Marguerite Madden:** Conceptualization, Funding acquisition, Investigation, Methodology, Supervision, Validation, Visualization, Writing – review & editing.

Ethics approval and consent to participate and publish

Not applicable.

Ethics in publishing statement

This research presents an accurate account of the work performed, all data presented are accurate and methodologies detailed enough to permit others to replicate the work.

This manuscript represents entirely original works and or if work and/or words of others have been used, that this has been appropriately cited or quoted and permission has been obtained where necessary.

This material has not been published in whole or in part elsewhere.

The manuscript is not currently being considered for publication in another journal.

That generative AI and AI-assisted technologies have not been utilized in the writing process or if used, disclosed in the manuscript the use of AI and AI-assisted technologies and a statement will appear in the published work.

That generative AI and AI-assisted technologies have not been used to create or alter images unless specifically used as part of the research design where such use must be described in a reproducible manner in the methods section.

All authors have been personally and actively involved in substantive work leading to the manuscript and will hold themselves jointly and individually responsible for its content.

Funding

This research was primarily funded by the National Program for Scientific Research and Advanced Studies (PROCIENCIA) through the Basic Research Project with contract No. PE501084701-2023-PROCIENCIA.

Declaration of competing interests

The authors declare that they have no known competing financial interests or personal relationships that could have appeared to influence the work reported in this paper.

Acknowledgments

We would like to thank the Center for Geospatial Research (CGR) at the University of Georgia (USA) for allowing us to carry out our research internship on “Crop monitoring in tropical ecosystems using remote sensing (NASA Sensors + SAR + UAV + LiDAR) and cloud computing.” We also thank the Geomatics Research Laboratory at the National University Toribio Rodríguez de Mendoza de Amazonas and the National Program for Scientific Research and Advanced Studies (PROCIENCIA).

Appendix B. Supplementary data

Supplementary data to this article can be found online at https://doi.org/10.1016/j.rsase.2026.102200.

Appendix A. Supplementary Material

Fig. S1: Determination of average monthly precipitation from 1981 to 2025 to identify the dry season and rainy season in a) the province of San Ignacio and b) Jaen; Fig. S2: Importance of variables according to the VIF test; Table S1: List of bands of Harmonized Sentinel-2 MSI: MultiSpectral Instrument, Level-2A (SR), before feature reduction. The bands were used for the dry and wet seasons; Table S2: List of indices and TCT used for station; Table S3: List of Sentinel-1 features, prior to feature reduction. Texture features and spatiotemporal metrics were calculated in a temporal composite for the entire time period for each year. Table S4. Confusion matrix for 2019–2024.

Data availability

The data that support the findings of this study are available at: https://doi.org/10.6084/m9.figshare.33102239.

References

Adrah, E., Wong, J.P., Yin, H., 2025. Integrating GEDI, Sentinel-2, and Sentinel-1 imagery for tree crops mapping. Rem. Sens. Environ. 319 (March), 7–9. https://doi.org/10.1016/j.rse.2025.114644.

Aires, U.R.V., Martins, V.S., Ferreira, L.B., Huang, Y., Heintzman, L., Ouyang, Y., 2025. Impact of sampling techniques on crop type mapping using multi-temporal composites from Harmonized landsat-sentinel images. Comput. Electron. Agric. 237 (October), 1–3. https://doi.org/10.1016/j.compag.2025.110676.

Avelino, J., Gagliardi, S., Perfecto, I., Isaac, M.E., Liebig, T., Vandermeer, J., Merle, I., Hajian-Forooshani, Z., Motisi, N., 2023. Tree effects on coffee leaf rust at field and landscape scales. Plant Dis. 107 (2), 247–261. https://doi.org/10.1094/PDIS-08-21-1804-FE.

Bahrami, H., McNairn, H., Mahdianpari, M., Homayouni, S., 2022. A meta-analysis of remote sensing technologies and methodologies for crop characterization. Remote Sens. 14 (22), 1–47. https://doi.org/10.3390/rs14225633.

Balling, J., Herold, M., Reiche, J., 2023. How textural features can improve SAR-based tropical forest disturbance mapping. Int. J. Appl. Earth Obs. Geoinf. 124 (June), 103492. https://doi.org/10.1016/j.jag.2023.103492.

Barboza, E., Salazar, W., Gálvez-Paucar, D., Valqui-Valqui, L., Valqui, L., Zagaceta, L.H., Gonzales, J., Vásquez, H.V., Arbizu, C.I., 2024. Cloud computing application for the analysis of land use and land cover changes in dry forests of Peru. Int. J. Environ. Impacts 7 (3), 505–514. https://doi.org/10.18280/ijei.070312.

Barboza, E., Turpo, E.Y., De Almeida, C.M., Salas, R., Rojas, N.B., Silva, J.O., Barrena, M.A., Oliva, M., Espinoza-Villar, R., 2020. Monitoring wildfires in the northeastern peruvian amazon using landsat-8 and sentinel-2 imagery in the GEE platform. ISPRS Int. J. GeoInf. 9 (10), 1–22. https://doi.org/10.3390/ijgi9100564.

Bernardes, T., Moreira, M.A., Adami, M., Giarolla, A., Rudorff, B.F.T., 2012. Monitoring biennial bearing effect on coffee yield using MODIS remote sensing imagery. Remote Sens. 4 (9), 2492–2509. https://doi.org/10.3390/rs4092492.

Bousbih, S., Zribi, M., Lili-Chabaane, Z., Baghdadi, N., El Hajj, M., Gao, Q., Mougenot, B., 2017. Potential of sentinel-1 radar data for the assessment of soil and cereal cover parameters. Sensors (Switzerland) 17 (11). https://doi.org/10.3390/s17112617.

Bouvet, A., Mermoz, S., Ballère, M., Koleck, T., Le Toan, T., 2018. Use of the SAR shadowing effect for deforestation detection with Sentinel-1 time series. Remote Sens. 10 (8), 1–19. https://doi.org/10.3390/rs10081250.

Breiman, Leo, 2001. Random Forests. Machine Learning 45 (1), 5–32. https://doi.org/10.1023/a:1010933404324. https://link.springer.com/10.1023/A:1010933404324.

Camino, C., Valero-Jorge, A., Lima, E.G., Álvarez, R., Beck, P.S.A., Álvarez-Taboada, F., 2025. Detection and monitoring of Melampsora spp. damage in multiclonal poplar plantations coupling biophysical models and Sentinel-2 time series. Int. J. Appl. Earth Obs. Geoinf. 141 (March). https://doi.org/10.1016/j.jag.2025.104663.

Chemura, A., Mutanga, O., Dube, T., 2017. Integrating age in the detection and mapping of incongruous patches in coffee (Coffea arabica) plantations using multi-temporal landsat 8 NDVI anomalies. Int. J. Appl. Earth Obs. Geoinf. 57, 1–13. https://doi.org/10.1016/j.jag.2016.12.007.

Chemura, A., Mutanga, O., Odindi, J., Kutywayo, D., 2018. Mapping spatial variability of foliar nitrogen in coffee (Coffea arabica L.) plantations with multispectral Sentinel-2 MSI data. ISPRS J. Photogrammetry Remote Sens. 138, 1–11. https://doi.org/10.1016/j.isprsjprs.2018.02.004.

Crawford, Christopher J., Manson, Steven M., Bauer, Marvin E., Hall, Dorothy K., 2013. Multitemporal snow cover mapping in mountainous terrain for Landsat climate data record development. Remote Sensing of Environment 135, 224–233. https://doi.org/10.1016/j.rse.2013.04.004. https://linkinghub.elsevier.com/retrieve/pii/S0034425713001259.

da Silva, P.C., Ribeiro Junior, W.Q., Ramos, M.L.G., Lopes, M.F., Santana, C.C., Casari, R.A., das, C.N., Brasileiro, L. de O., Veiga, A.D., Rocha, O.C., Malaquias, J.V., Souza, N.O.S., Roig, H.L., 2024. Multispectral images for drought stress evaluation of Arabica coffee genotypes under different irrigation regimes. Sensors 24 (22), 1–23. https://doi.org/10.3390/s24227271.

Dormann, C.F., Elith, J., Bacher, S., Buchmann, C., Carl, G., Carré, G., Marquéz, J.R.G., Gruber, B., Lafourcade, B., Leitão, P.J., Münkemüller, T., Mcclean, C., Osborne, P.E., Reineking, B., Schröder, B., Skidmore, A.K., Zurell, D., Lautenbach, S., 2013. Collinearity: a review of methods to deal with it and a simulation study evaluating their performance. Ecography 36 (1), 27–46. https://doi.org/10.1111/j.1600-0587.2012.07348.x.

Drielsma, M.J., Love, J., Taylor, S., Thapa, R., Williams, K.J., 2022. General Landscape Connectivity Model (GLCM): a new way to map whole of landscape biodiversity functional connectivity for operational planning and reporting. Ecol. Model. 465, 109858. https://doi.org/10.1016/j.ecolmodel.2021.109858.

Ehrenbergerová, L., Klimková, M., Cano, Y.G., Habrová, H., Lvončík, S., Volařík, D., Khum, W., Němec, P., Kim, S., Jelínek, P., Maděra, P., 2021. Does shade impact coffee yield, tree trunk, and soil moisture on coffea canephora plantations in Mondulkiri, Cambodia? Sustainability 13 (24). https://doi.org/10.3390/su132413823.

Escobar-López, A., Castillo-Santiago, M.Á., Hernández-Stefanoni, J.L., Mas, J.F., López-Martínez, J.O., 2022. Identifying coffee agroforestry system types using multitemporal Sentinel-2 data and auxiliary information. Remote Sens. 14 (16), 1–15. https://doi.org/10.3390/rs14163847.

Farr, T.G., Rosen, P.A., Caro, E., Crippen, R., Duren, R., Hensley, S., Kobrick, M., Paller, M., Rodriguez, E., Roth, L., Seal, D., Shaffer, S., Shimada, J., Umland, J., Werner, M., Oskin, M., Burbank, D., Alsdorf, D., 2007. The shuttle radar topography Mission. Rev. Geophys. 45 (RG2004), 1–33. https://doi.org/10.1029/2005RG000183.

Fekadu, A., Andarege, B., 2025. Gis and parametric based coffee site suitability zonation in North Shewa zone of Oromia region, central Ethiopia. Environ. Sustain. Indic. 26 (March). https://doi.org/10.1016/j.indic.2025.100674.

Gorelick, N., Hancher, M., Dixon, M., Ilyushchenko, S., Thau, D., Moore, R., 2017. Google Earth engine: planetary-scale geospatial analysis for everyone. Rem. Sens. Environ. 202, 18–27. https://doi.org/10.1016/j.rse.2017.06.031.

Haralick, R.M., Dinstein, I., Shanmugam, K., 1973. Textural features for image classification. IEEE Trans. Syst. Man Cybern. SMC-3 (6), 610–621. https://doi.org/10.1109/TSMC.1973.4309314.

Hasanuzzaman, M., Pratim Adhikary, P., Kumar, Shit P., 2024. Gully erosion susceptibility mapping and prioritization of gully-dominant sub-watersheds using machine learning algorithms: evidence from the Silabati river (tropical river, India). Adv. Space Res. 73 (3), 1653–1666. https://doi.org/10.1016/j.asr.2023.10.051.

Hegazy, I.R., Kaloop, M.R., 2015. Monitoring urban growth and land use change detection with GIS and remote sensing techniques in Daqahlia governorate Egypt. Int. J. Sustain. Built Environ. 4 (1), 117–124. https://doi.org/10.1016/j.ijsbe.2015.02.005.

Housman, I.W., Chastain, R.A., Finco, M.V., 2018. An evaluation of forest health insect and disease survey data and satellite-based remote sensing forest change detection methods: case studies in the United States. Remote Sens. 10 (8). https://doi.org/10.3390/rs10081184.

Hu, L., Li, W., Xu, B., 2018. Monitoring mangrove forest change in China from 1990 to 2015 using Landsat-derived spectral-temporal variability metrics. Int. J. Appl. Earth Obs. Geoinf. 73 (19), 88–98. https://doi.org/10.1016/j.jag.2018.04.001.

Ibrahim, E.S., Rufin, P., Nill, L., Kamali, B., Nendel, C., Hostert, P., 2021. Mapping crop types and cropping systems in Nigeria with sentinel-2 imagery. Remote Sens. 13 (17), 1–24. https://doi.org/10.3390/rs13173523.

INEI, 2022. Perú: proyecciones de población, según departamento, provincia y distrito, 2018-2020. In: Informes Y Publicaciones. *Boletín es*. https://www.gob.pe/institucion/inei/informes-publicaciones/3464927-peru-proyecciones-de-poblacion-total-segun-departamento-provincia-y-distrito-2018-2022.

JNC, 2020. El café de Perú. Junta Nacional Del Café 1. El café en el Perú.

Julca-Otiniano, A., Alvarado-Huamán, L., Borjas-Ventura, R., Castro-Cepero, V., León Rojas, F., Valderrama Palacios, D., Bello Amez, S., 2023. Variedades de café (Coffea arabica), una revisión y algunas experiencias en el Perú. Revista de Investigación e Innovación Agropecuaria y de Recursos Naturales 10 (2). https://doi.org/10.53287/ruyx4519vm15b.

Kawakubo, F.S., Pérez Machado, R.P., 2016. Mapping coffee crops in southeastern Brazil using spectral mixture analysis and data mining classification. Int. J. Rem. Sens. 37 (14), 3414–3436. https://doi.org/10.1080/01431161.2016.1201226.

Kelley, L.C., Pitcher, L., Bacon, C., 2018. Using google earth engine to map complex shade-grown coffee landscapes in northern Nicaragua. Remote Sens. 10 (6). https://doi.org/10.3390/rs10060952.

Klehr, D., Stoffels, J., Hill, A., Pham, V.D., van der Linden, S., Frantz, D., 2025. Mapping tree species fractions in temperate mixed forests using Sentinel-2 time series and synthetically mixed training data. Rem. Sens. Environ. 323 (October 2024), 114740. https://doi.org/10.1016/j.rse.2025.114740.

Le, Q.T., Dang, K.B., Giang, T.L., Tong, T.H.A., Nguyen, V.G., Nguyen, T.D.L., Yasir, M., 2022. Deep learning model development for detecting coffee tree changes based on Sentinel-2 imagery in Vietnam. IEEE Access 10 (August), 109097–109107. https://doi.org/10.1109/ACCESS.2022.3203405.

Lelong, C.C.D., Thong-Chane, A., 2003. Application of textural analysis on very high resolution panchromatic images to map coffee orchards in Uganda. Int. Geosci. Remote Sensing Sympos. (IGARSS) 2 (C), 1007–1009. https://doi.org/10.1109/igarss.2003.1293994.

Liu, X., Frey, J., Munteanu, C., Still, N., Koch, B., 2023. Mapping tree species diversity in temperate montane forests using Sentinel-1 and Sentinel-2 imagery and topography data. Rem. Sens. Environ. 292 (July), 113576. https://doi.org/10.1016/j.rse.2023.113576.

Liu, X., Tan, Y., Dong, J., Wu, J., Wang, X., Sun, Z., 2025. Assessing habitat selection parameters of Arabica coffee using BWM and BCM methods based on GIS. Sci. Rep. 15 (1), 1–19. https://doi.org/10.1038/s41598-024-84073-0.

Liu, Y., Gong, W., Hu, X., Gong, J., 2018. Forest type identification with random forest using Sentinel-1A, Sentinel-2A, multi-temporal Landsat-8 and DEM data. Remote Sens. 10 (6), 1–25. https://doi.org/10.3390/rs10060946.

Mansaray, L.R., Wang, F., Huang, J., Yang, L., Kanu, A.S., 2020. Accuracies of support vector machine and random forest in rice mapping with Sentinel-1A, Landsat-8 and Sentinel-2A datasets. Geocarto Int. 35 (10), 1088–1108. https://doi.org/10.1080/10106049.2019.1568586.

Marin, D.B., Ferraz, G.A.e.S., Santana, L.S., Barbosa, B.D.S., Barata, R.A.P., Osco, L.P., Ramos, A.P.M., Guimarães, P.H.S., 2021. Detecting coffee leaf rust with UAV-based vegetation indices and decision tree machine learning models. Comput. Electron. Agric. 190 (September). https://doi.org/10.1016/j.compag.2021.106476.

Maskell, G., Chemura, A., Nguyen, H., Gornott, C., Mondal, P., 2021. Integration of sentinel optical and radar data for mapping smallholder coffee production systems in Vietnam. Rem. Sens. Environ. 266 (September), 112709. https://doi.org/10.1016/j.rse.2021.112709.

Masolele, R.N., De Sy, V., Marcos, D., Verbesselt, J., Gieseke, F., Mulatu, K.A., Moges, Y., Sebrala, H., Martius, C., Herold, M., 2022. Using high-resolution imagery and deep learning to classify land-use following deforestation: a case study in Ethiopia. GIScience Remote Sens. 59 (1), 1446–1472. https://doi.org/10.1080/15481603.2022.2115619.

Medina, A.J., López, R.S., Zabaleta-santisteban, J.A., Tuesta-trauco, K.M., Rivera-fernández, A.S., Sánchez, J.A., Silva-melendez, T.B., Silva-lópez, J.O., Rojas, N.B., Alberca, M.A.G., Díaz, C.P., Cruz, M.O., Barboza, E., Silva-lópez, J.O., Briceno, N.B.R., Alberca, M.A.G., 2026. Integration of sentinel optical and radar data in Google Earth Engine for mapping small complex agroforests of shade-grown coffee in northern Peru, 6049. https://doi.org/10.1080/10106049.2025.2596243.

Medina Medina, A.J., Salas López, R., Zabaleta Santisteban, J.A., Tuesta Trauco, K.M., Turpo Cayo, E.Y., Huaman Haro, N., Oliva Cruz, M., Gómez Fernández, D., 2024. An analysis of the rice-cultivation dynamics in the lower utcubamba River Basin using SAR and optical imagery in Google Earth Engine (GEE). Agronomy 14 (3), 557. https://doi.org/10.3390/agronomy14030557.

MINAGRI, 2018. Plan Nacional De Acción Del Cafe Peruano 2018-2030. Plan Nacional De Accion Del Café 1, 53.

Mishra, V.N., Prasad, R., Rai, P.K., Vishwakarma, A.K., Arora, A., 2019. Performance evaluation of textural features in improving land use/land cover classification accuracy of heterogeneous landscape using multi-sensor remote sensing data. Earth Sci. Inf. 12 (1), 71–86. https://doi.org/10.1007/s12145-018-0369-z.

Moreira, E.P., Valeriano, M.M., 2014. Application and evaluation of topographic correction methods to improve land cover mapping using object-based classification. Int. J. Appl. Earth Obs. Geoinf. 32 (1), 208–217. https://doi.org/10.1016/j.jag.2014.04.006.

Müller, H., Rufin, P., Griffiths, P., Barros Siqueira, A.J., Hostert, P., 2015. Mining dense landsat time series for separating cropland and pasture in a heterogeneous Brazilian savanna landscape. Rem. Sens. Environ. 156, 490–499. https://doi.org/10.1016/j.rse.2014.10.014.

Nguyen, M.D., Baez-Villanueva, O.M., Bui, D.D., Nguyen, P.T., Ribbe, L., 2020. Harmonization of landsat and sentinel 2 for crop monitoring in drought prone areas: case studies of Ninh Thuan (Vietnam) and Bekaa (Lebanon). Remote Sens. 12 (2), 1–18. https://doi.org/10.3390/rs12020281.

Nogueira, S.M.C., Moreira, M.A., Volpato, M.M.L., 2018. Relationship between coffee crop productivity and vegetation indexes derived from oli/landsat-8 sensor data with and without topographic correction. Int. Brazi. Assoc. Agric. Eng. 38 (3), 387–394. https://doi.org/10.1590/1809-4430-Eng.Agric.v38n3p387-394/2018RELATIONSHIP.

Numbisi, F.N., Van Coillie, F.M.B., De Wulf, R., 2019. Delineation of cocoa agroforests using Multiseason Sentinel-1 SAR images: a low grey level range reduces uncertainties in GLCM texture-based mapping. ISPRS Int. J. GeoInf. 8 (4), 179. https://doi.org/10.3390/ijgi8040179.

O'brien, R.M., 2007. A caution regarding rules of thumb for variance inflation factors. Qual. Quantity 41 (5), 673–690. https://doi.org/10.1007/s11135-006-9018-6.

Ocaña-Zuñiga, C., Quiñones-Huatangari, L., Barboza, E., Peña, N.C., Zamora, S.H., Ojeda, J.M.P., 2025. Coffee rust severity analysis in agroforestry systems using deep learning in Peruvian tropical ecosystems. Agriculture (Switzerland) 15 (1), 35. https://doi.org/10.3390/agriculture15010039.

Ortega-Huerta, M.A., Komar, O., Price, K.P., Ventura, H.J., 2012. Mapping coffee plantations with land sat imagery: an example from El Salvador. Int. J. Rem. Sens. 33 (1), 220–242. https://doi.org/10.1080/01431161.2011.591442.

Poortinga, A., Tenneson, K., Shapiro, A., Nquyen, Q., Aung, K.S., Chishtie, F., Saah, D., 2019. Mapping plantations in Myanmar by fusing Landsat-8, Sentinel-2 and Sentinel-1 data along with systematic error quantification. Remote Sens. 11 (7), 1–19. https://doi.org/10.3390/rs11070831.

Putra, B.T.W., Soni, P., Marhaenanto, B., Pujiyanto, Sisbudi Harsono, S., Fountas, S., 2020. Using information from images for plantation monitoring: a review of solutions for smallholders. Inf. Process. Agric. 7 (1), 109–119. https://doi.org/10.1016/j.inpa.2019.04.005.

Qiu, B., Hu, X., Chen, C., Tang, Z., Yang, P., Zhu, X., Yan, C., Jian, Z., 2022. Maps of cropping patterns in China during 2015–2021. Sci. Data 9 (1), 1–9. https://doi.org/10.1038/s41597-022-01589-8.

Qiu, B., Li, Z., Yang, P., Wu, W., Chen, X., Wu, B., Zhang, M., Duan, Y., Kurniawan, S., Tryjanowski, P., Takacs, V., 2025. Towards automation of national scale cropping pattern mapping by coupling Sentinel-1/2 data: a 10-m map of crop rotation systems for wheat in China. Agric. Syst. 227 (June), 1–7. https://doi.org/10.1016/j.agsy.2025.104338.

Saad, H., El Harti, A., Panimboza, J., 2022. Investigating Sentinel-1 and Sentinel-2 data efficiency in studying the temporal behavior of wheat phenological stages using Google Earth engine. Agriculture (Switzerland) 12 (10), 1–27. https://doi.org/10.3390/agriculture12101605.

Salas, R., Fernández, D.G., Silva, J.O., Rojas, N.B., Oliva, M., Terrones Murga, R.E., Trigoso, D.I., Barboza, E., Barrena, M.Á., 2020. Land suitability for coffee (coffea arabica) growing in Amazonas, Peru: integrated use of AHP, GIS and RS. ISPRS Int. J. GeoInf. 9 (11), 1–21. https://doi.org/10.3390/ijgi9110673.

Schmitt, M., Hughes, L.H., Qiu, C., Zhu, X.X., 2019. AGGREGATING CLOUD-FREE SENTINEL-2 IMAGES with GOOGLE EARTH ENGINE. ISPRS Annals of the Photogrammetry, Remote Sensing and Spatial Information Sciences 4 (2/W7), 145–152. https://doi.org/10.5194/isprs-annals-IV-2-W7-145-2019.

Schulz, C., Förster, M., Vulova, S.V., Rocha, A.D., Kleinschmit, B., 2024. Spectral-temporal traits in Sentinel-1 C-band SAR and Sentinel-2 multispectral remote sensing time series for 61 tree species in Central Europe. Rem. Sens. Environ. 307 (April). https://doi.org/10.1016/j.rse.2024.114162.

SENAMHI, 2020. Caracterización y zonificación por aptitud agroclimática del cultivo de Café. Repositorio Institucional - SENAMHI 1, 55.

Shi, T., Xu, H., 2019. Derivation of tasseled cap transformation coefficients for Sentinel-2 MSI At-Sensor reflectance data. IEEE J. Sel. Top. Appl. Earth Obs. Remote Sens. 12 (10), 4038–4048. https://doi.org/10.1109/JSTARS.2019.2938388.

Silva, W.F., Rudorff, B.F.T., Formaggio, A.R., Paradella, W.R., Mura, J.C., 2009. Discrimination of agricultural crops in a tropical semi-arid region of Brazil based on L-band polarimetric airborne SAR data. ISPRS J. Photogrammetry Remote Sens. 64 (5), 458–463. https://doi.org/10.1016/j.isprsjprs.2008.07.005.

Somarriba, E., Saj, S., Orozco-Aguilar, L., Somarriba, A., Rapidel, B., 2024. Shade canopy density variables in cocoa and coffee agroforestry systems. Agrofor. Syst. 98 (3), 585–601. https://doi.org/10.1007/s10457-023-00931-2.

Son, N.T., Chen, C.F., Chen, C.R., Cheng, Y.S., Chen, S.H., 2023. Multidecadal evaluation of changes in coffee-growing areas using Landsat data in central highlands, Vietnam. Geocarto Int. 38 (1). https://doi.org/10.1080/10106049.2023.2204099.

Tamiminia, H., Salehi, B., Mahdianpari, M., Quackenbush, L., Adeli, S., Brisco, B., 2020. Google Earth Engine for geo-big data applications : a meta-analysis and systematic review. ISPRS J. Photogrammetry Remote Sens. 164 (January), 152–170. https://doi.org/10.1016/j.isprsjprs.2020.04.001.

Tassew, A.A., Yadessa, G.B., Bote, A.D., Obso, T.K., 2021. Influence of location, elevation gradients, processing methods, and soil quality on the physical and cup quality of coffee in the Kafa Biosphere reserve of SW Ethiopia. Heliyon 7 (8), e07790. https://doi.org/10.1016/j.heliyon.2021.e07790.

Torres, N.E., Melchor-Martínez, E.M., Ochoa Sierra, J.S., Ramirez-Mendoza, R.A., Parra-Saldívar, R., Iqbal, H.M.N., 2020. Impact of climate change and early development of coffee rust – an overview of control strategies to preserve organic cultivars in Mexico. Sci. Total Environ. 738, 140225. https://doi.org/10.1016/j.scitotenv.2020.140225.

Tridawati, A., Wikantika, K., Susantoro, T.M., Harto, A.B., 2020. Mapping the distribution of Co ff ee plantations from data using a random forest algorithm. Remote Sens. 12.

Turpo, E.Y., Borja, M.O., Espinoza-Villar, R., Moreno, N., Camargo, R., Almeida, C., Hopfgartner, K., Yarleque, C., Souza, C.M., 2022. Mapping three decades of changes in the tropical andean glaciers using landsat data processed in the Earth engine. Remote Sens. 14 (9). https://doi.org/10.3390/rs14091974.

Wachowiak, M.P., Walters, D.F., Kovacs, J.M., Wachowiak-Smolíková, R., James, A.L., 2017. Visual analytics and remote sensing imagery to support community-based research for precision agriculture in emerging areas. Comput. Electron. Agric. 143, 149–164. https://doi.org/10.1016/j.compag.2017.09.035.

Waldner, F., Chen, Y., Lawes, R., Hochman, Z., 2019. Needle in a haystack: mapping rare and infrequent crops using satellite imagery and data balancing methods. Rem. Sens. Environ. 233 (September), 111375. https://doi.org/10.1016/j.rse.2019.111375.

Widjaya, Dani, Yanuarti, Rizky, 2024. Mapping coffee base countries in the world: Case studies from three continents (Africa-America-Asia). Pelita Perkebunan (a Coffee and Cocoa Research Journal) 40 (1), 61–75. https://doi.org/10.22302/iccri.jur.pelitaperkebunan.v40i1.593. https://www.ccrjournal.com/index.php/ccrj/article/view/593. (Accessed 29 April 2024).

Zhao, R., You, W., Fan, D., 2024. Staple crop mapping potential analysis and application of Sentinel-1 interferometric coherence: a case study in the Songnen Plain, China. Adv. Space Res. 74 (7), 2993–3010. https://doi.org/10.1016/j.asr.2024.06.037.